Spectrometer for the Study of Angle- and Energy-Resolved Reactive Ion Scattering at Surfaces

S-J. Han, C.-W. Lee, C.-H. Hwang, K.-H. Lee, M. C. Yang, and H. Kang[*,†]

Department of Chemistry, Pohang University of Science and Technology, Pohang 790-784, Korea
[†]Department of Chemistry and Center for Ion-Surface Reaction, Seoul National University, Seoul 151-742, Korea
Received May 21, 2001

We describe an ion-surface scattering apparatus newly developed to investigate the reactive scattering process of low-energy alkali-metal ions at surfaces. The apparatus consists of an alkali-metal ion gun that is rotatable by 360°, a quadrupole mass spectrometer (QMS) with an ion energy analyzer, a sample manipulator with a heating-and-cooling stage, and an ultrahigh vacuum (UHV) chamber that houses these components. Preliminary experimental results obtained from the apparatus are presented on angular and energy distributions of the ions scattered from clean Pt(111) and water-adsorbed Pt surfaces.

Keywords : Ion-surface scattering, Alkali metal, Platinum, Surface analysis.

Introduction

Interactions of low energy (5-100 eV) ions with solid surfaces have emerged as an important research subject. In particular, reactive ion projectiles often induce new and intriguing chemical processes upon surface collision: a molecular projectile ion can undergo dissociation, transfer its functional group to a surface, be deposited as a film, or pick up a surface species upon scattering. A range of phenomena associated with low-energy reactive ion-surface collisions have been reviewed.[1,2] Among these, the phenomena that projectile ions pick up surface molecules or exchange functional groups with a surface, often called reactive ion scattering (RIS), have been actively investigated owing to its potential application to surface analysis.[3-13]

Recently we have observed a unique RIS process of low-energy Cs^+ ions, in which Cs^+ picks up a surface molecule (X) to form a CsX^- cluster ion upon scattering.[5-7] Cs^+ is chemically inert and binds with a gas-phase molecule through purely electrostatic interaction, *i.e.*, the ion-molecule attraction force. This feature suggests non-specificity of the RIS process in picking up a variety of adsorbed molecules, or universal applicability for surface analysis. Since Cs^- undergoes little ion neutralization upon surface scattering due to its low ionization energy, the scattered ions can be detected with high sensitivity. Several case studies to date showed that it is indeed possible to identify surface molecules and functional groups by this method.[5-13] The systems examined include chemisorbed species (CO, O_2, O atom, Cs atom, OH, water, ethyl group, and benzene) on surfaces,[5-11] physisorbed molecules (ethylene, disilabutane, and water),[10-12] as well as multilayer films of ice and chemical species deposited on them.[12,13]

To the present Cs^- RIS studies have been performed with an instrument designed for fixed scattering angle experiment.[14] Mechanistic study of the RIS process in this configuration[6,7] suggests a two-step mechanism: incident Cs^+ ions induce collisional desorption of molecules, and then Cs^--molecule complexes are formed *via* ion-molecule associative reaction in the gas phase. There are, however, many features still uncertain for the mechanism, such as the collision dynamics between a Cs^+ projectile and a molecule on surface at such low incident energies as well as the nature of reactive process resulting from the collision. The RIS process may differ in nature from one type of surface to another, as already indicated by the drastically different RIS yields observed from chemisorbed molecules[5-11] and ice films.[12,13] To gain better understanding of the RIS process, and to improve the control over experimental parameters, it is necessary to undertake experiment in which both incident and scattering angles are varied. The energy of scattered ions can reveal additional important information. In this article, we describe an instrument designed and built for such experiment, which has ability to independently control incident and scattering angles. RIS products leaving a surface are analyzed for their kinetic energy as well as their mass-to-charge ratio using a QMS equipped with an energy analyzer. We demonstrate how these new features allow one to explore the ion-surface scattering and RIS processes.

Instrument

UHV scattering chamber. The basic units of the apparatus are a UHV scattering chamber, a rotatable ion source, and a QMS detector. The scattering chamber, shown in Figure 1 for an overview, was designed in the laboratory and manufactured by MDC Vacuum Products.[15] The chamber consists of two working levels. The upper level, designed as a standard surface science chamber, serves for sample preparation and characterization. It contains a cylindrical mirror analyzer (CMA) with a coaxial electron gun for Auger electron spectroscopy (AES), a sputter ion gun for surface cleaning, and a few spare flanges that can be used for other

*Corresponding author: Tel: +82-2-875-7471, Fax: +82-2-889-5719, e-mail: surfion@snu.ac.kr

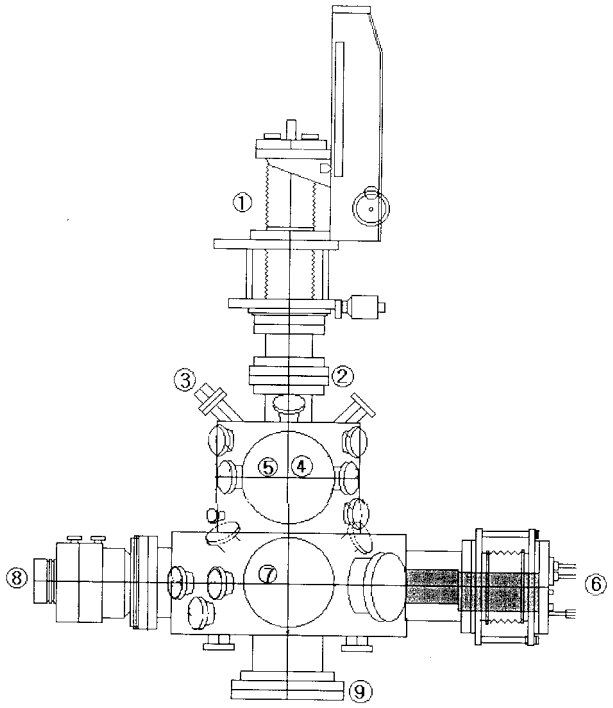

Figure 1. Overview of the angle-resolved reactive ion scattering chamber. The labeled components are: ① sample manipulator (x, y, z-motion), ② rotatable flange, ③ sputter ion gun, ④ view port, ⑤ CMA for AES (back side), ⑥ QMS, ⑦ view port, ⑧ TMP, ⑨ rotatable flange (ion gun stage).

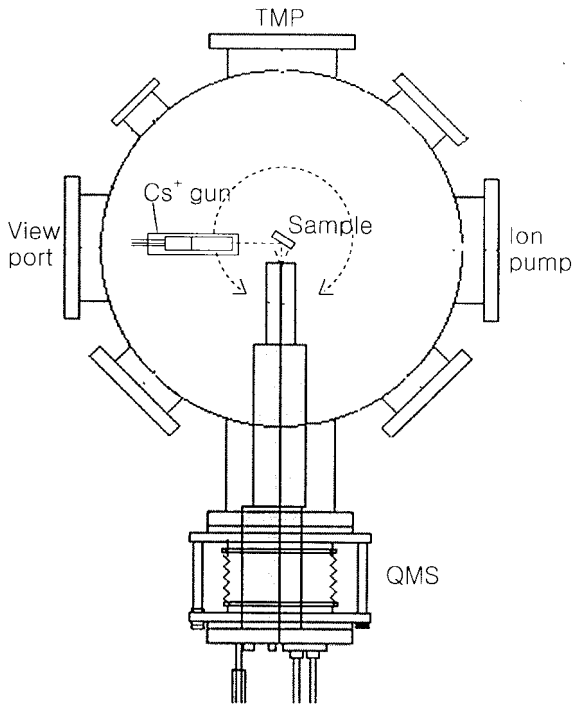

Figure 2. Components in the lower level of the spectrometer chamber (top view).

spectroscopic tools. The AES is installed on a bellowed flange of 15 cm in diameter which can travel up to 5 cm. The lower level, shown in Figure 2, houses the components for angle-resolved RIS experiment, including a rotatable Cs^+ ion gun (Kimball Physics[16]) and a QMS (ABB Extrel, model MEXM1000[17]). The lower level has a larger diameter (50 cm) than the upper level (30.5 cm) to provide a room for Cs^+ gun rotation. A turbomolecular pump (TMP, 360 L/sec) and an ion pump (500 L/sec) are in the lower level to maintain the chamber base-pressure at 5×10^{-11} Torr. The overall height of the chamber is 144 cm including the length of a long-travel sample manipulator. A small crane, installed at the ceiling above the chamber, is used to lift the sample manipulator and transport it to a work bench located nearby.

A target is positioned at the center of a scattering chamber, and motion is possible in three translational degrees of freedom (5 cm in x and y and 30 cm in z) and in rotation around the z axis by using a sample manipulator installed on a rotary flange. The long travel distance in z allows the target to move between the lower and upper levels. The target can be heated or cooled for sample preparation and for variable-temperature experiment using a home-built heating-and-cooling stage. In this stage, a cryogenic cold finger made of oxygen-free high-conductivity (OFHC) copper stores liquid nitrogen and is maintained at 77.4 K. The sample makes a thermal contact to the cold finger through sapphire plates with thickness of 0.5 mm, and thus the sample is electrically isolated from the copper. The sample can be heated by passing electric currents through heater filaments (resistive heating). The heater filaments are Ta wires of 0.4-0.5 mm in diameter and are symmetrically attached to the sides or back of a metal sample. To heat a semiconductor sample, we sandwich Ta foils between two flat samples and pass currents through the foils, which provides efficient radiative and resistive heating of the samples.[18] The currents through the filaments are provided by a DC power supply (Kepco, model ATE36-30M[19]), which is driven by a programmable Proportional-Integral-Derivative (PID) controller (Eurotherm, model 903P[20]). The design allows a sample not only to be maintained at a constant temperature, but also to be heated and cooled in a programmed way for temperature-dependent experiment and sample annealing. The sample temperature is variable in the range of 90-1500 K as read by a K-type thermocouple. The chamber pressure remains below 3×10^{-10} Torr even during sample flashing and annealing processes. A combined method of sample heating and Ar^+ ion sputtering at 2 keV provides an appropriate means for cleaning most of elemental samples. Cleanness of a surface is checked by AES and RIS. While AES is a preferred method to check elemental impurities such as surface carbons owing to its high sensitivity, RIS is more effective for detecting molecules adsorbed from chamber residual gases such as CO and water.

Ion source. Figure 2 shows components of the angle-resolved RIS instrument contained in the lower level of chamber. The two key components are a low-energy Cs^- ion gun mounted on a rotatable stage and a QMS that has an ion energy analyzer at its nose. The low-energy Cs^- gun, a custom-made version from Kimball Physics, employs a surface ionization source. It produces a Cs^- beam with

energy of 5-1000 eV and delivers a beam current of up to 1 microamp to a target in a focused spot of 1 mm in diameter, when the distance from the gun to a target is 3 cm. The Cs^+ current decreases rapidly as the beam energy is decreased below 20 eV due to the space charge effect, which is a common phenomenon for a low-energy ion gun employing simple ion optics lenses.[14] The beam intensity is more than enough for the purpose of RIS experiment which runs typically at a beam current of 1-30 nA at energy of 10-50 eV. The total length of the Cs^- gun is 10 cm, including the source, focusing lenses, and deflectors. Several versions of Cs^- gun were designed and constructed in our laboratory using a Cs^+ cartridge (Kimball Physics[16]), which showed a satisfactory performance at low energy.

Ion beam current at a target is measured by a picoammeter (Keithley, model 485[21]). For alkali ion beams, the nominal current measured at a flat target surface is often far smaller than the total ion flux reaching the target, because a large portion of the beam does not get neutralized at the surface and just scatters out as ions. The total ion flux is the quantity of relevance in RIS study, and this can be correctly measured by using a Faraday cup carefully designed such that it collects most of the ions that enter the cup. We prepared such a Faraday cup with a small aperture (1 mm in diameter) and placed it close to a sample in order to measure both the density and the spatial distribution of a Cs^- beam.

To perform an angle-resolved ion scattering experiment, we rotate a Cs^+ gun around a target that is also rotatable by 360°, while a QMS detector is held at a fixed position. This rather unique instrumental configuration, first employed by Yarmoff and coworkers for ion scattering experiment.[22,23] is easier to use than other designs because the alkali metal ion gun has a small size and does not require differential pumping. The gun is mounted on a stainless steel arm that is welded to a rotary platform located at the bottom of the chamber (Figure 3). The rotary platform is a UHV flange of outer diameter of 20 cm (MDC vacuum, model RMTG-450[15]) with a rotating shaft that is vacuum-sealed by Teflon cylinders and differential pumping. The gun, the mounting system, and the electrical wiring are all connected to this flange and move together during rotation to prevent them from being entangled. The independent rotary motions of a gun and a sample allow one to measure scattering events occurring at various angles. Due to shadowing of the beam by the QMS nose, scattering angles between 0 and 30° are not accessible to the detector.

QMS detector. Ions scattered from a target surface are analyzed for mass by a QMS which has a range of 1-1000 amu/charge. The QMS system has an electron impact ionizer and an axial energy analyzer (AEA; Bessel filter) in tandem in front of a quadrupole mass filter. In RIS experiment, the ionizer filament is switched off and the lens potentials are adjusted for efficient transmission of scattered ions. Kinetic energy of ions is measured by AEA. QMS can be operated in a number of modes depending on the information desired. To measure a kinetic energy distribution of specific ions, we fix the quadrupole filter to selectively transmit ions of a particular mass-to-charge ratio, and scan the energy analyzer. Holding the energy analyzer fixed while scanning the quadrupole filter yields a mass spectrum of ions with a particular kinetic energy window. If a mass spectrum is desired without prior energy analysis, we operate the energy filter at a maximum bandpass condition. Even in this mode some kinetic energy selection and ion discrimination may occur, and thus quantitative interpretation of mass spectral intensity requires certain cautions. For experiments that require the highest signal sensitivity, we just remove AEA from QMS, which increases the signal intensity by at least 20 times. Ions with different masses up to five can be monitored for their intensity variation in real-time (multiple ion monitoring). Ions that pass through a quadrupole filter are detected by an electron multiplier, which permits both positive and negative ion counting with high sensitivity. QMS also has a dynode secondary electron detector and a Faraday cage for low-sensitivity detection of ions.

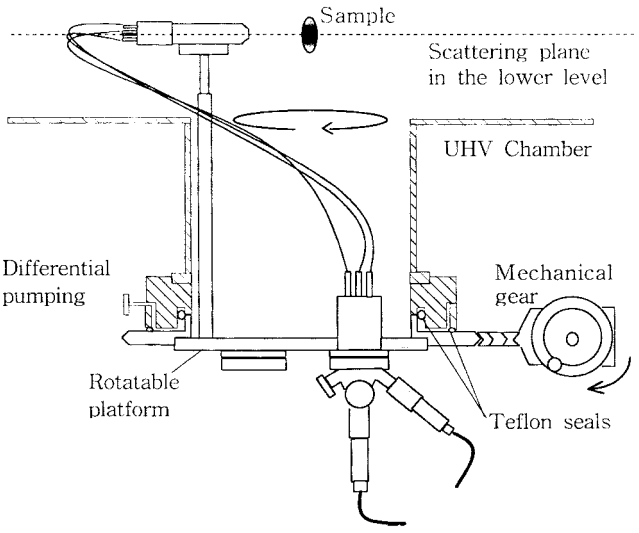

Figure 3. Cs^- ion gun mounted on a rotating flange. The ion gun rotates on a scattering plane defined by the positions of the gun, sample center, and QMS.

AEA is composed of an entrance electrode, a disk with a center hole, a main cylinder, and a blocking electrode located at the center of the main cylinder, and an exit electrode. A kinetic energy distribution measured by AEA was calibrated by using a Cs^+ beam of known energy. To do this, we pointed a Cs^- gun directly to the axis of AEA and quadrupole rods. Note that the gun is 360° rotatable. We then set the potential at the main cylinder to the known energy of Cs^- (5-300 eV), and tuned the potentials at the entrance and exit electrodes to optimize the ion transmission efficiency and the energy resolution. Once calibrated, only the potential of the main cylinder needs to be changed for ion energy analysis in most cases. Applying a more negative potential at the entrance electrode increases the efficiency of ion transmission, but at the same time decreases the energy resolution.

In RIS experiment, it is important to keep the scattering region around a target free of stray electric fields. The

scattered ions, in particular the RIS products, have very low kinetic energy, and their trajectories are easily disturbed by the presence of external electric fields from QMS ionizer and sample heater filaments. The noses of the QMS and the Cs^- gun are covered with electrical shields at the ground potential for this reason. Another important requirement for the experiment is proper alignment of an incident beam, a target, and a detector. The alignment condition may affect the intensity ratio of RIS products and is even more critical for ion energy analysis by AEA. The best geometry for the energy analysis is believed to be the one having line-of-sight transmission from a target through the quadrupole axis, which can be attained by aligning the components with the eyes and optical means through extra view ports available in the chamber.

Instrument Performance

The instrument has a capability to measure both mass and kinetic energy of scattered ions. This capability, when combined with wide ranges of collision energy and scattering angle available, allows many different types of experiment to be performed. In the following sections we report preliminary results of these experiments. A "non-reactive" scattering study of a Cs^+ beam was performed on a bare (111) surface of a Pt single crystal. For a reactive scattering experiment, we adsorbed water and carbon monoxide molecules on the Pt surface and investigated the pickup of these molecules by Cs^-.

RIS mass spectrum. In many cases the prime purpose of Cs^- RIS experiment is to identify chemical species on surfaces, which can be done simply by analyzing the mass of scattered CsX^+ ions. Figure 4 shows a positive ion mass spectrum of the species scattered from a Pt(111) surface covered with CO and H_2O. CO was adsorbed on the surface by introducing CO gas into the chamber for about 2 L at the sample temperature of 200 K. H_2O was adsorbed from the residual H_2O gas in the chamber by leaving the sample some time in UHV. The strongest peak seen in the spectrum is Cs^- ions elastically (non-reactively) scattered from the surface, appeared at m/z = 133 amu/charge. The intensity of this peak is shown in a reduced scale. Two additional peaks observed are due to reactive ion scattering: the peak at m/z = 151 amu/charge (CsH_2O^+) is due to pickup of H_2O from the surface and that at m/z = 161 amu/charge ($CsCO^+$) is due to pickup of CO. These RIS peaks confirm that H_2O and CO adsorb in the molecular states on a Pt(111) surface.[24] The absence of fragmentation peaks of these molecules ($CsOH^+$, CsO^+, and etc.) indicates that the molecules are desorbed intact by the Cs^+ collision. It also indicates that the Pt surface is not contaminated with Cs from the beam: in the presence of Cs impurity on Pt, certain portions of H_2O and CO will dissociate into OH, O, and C.[7]

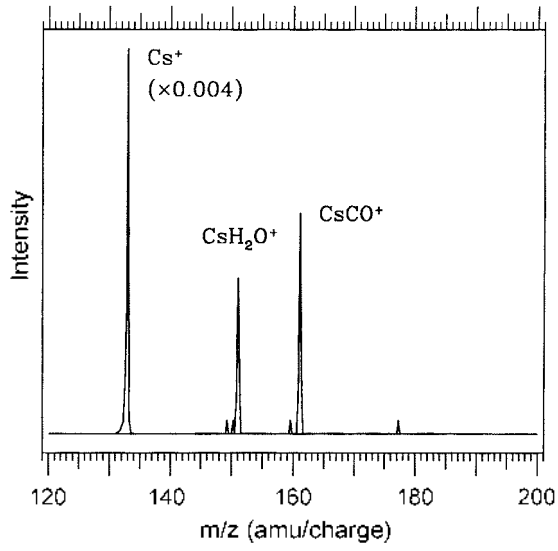

Figure 4. RIS mass spectrum obtained on a Pt surface adsorbed with CO and H_2O. A clean Pt(111) surface was exposed to CO gas for 2 L at 200 K, and H_2O was adsorbed from the residual water vapor inside the chamber. The incidence/exit angles were 45°/45° to the surface plane. Cs^+ beam energy was 10 eV. The spectrum was taken with AEA detached from QMS. The height of Cs^- peak was reduced by a factor of 0.004. The features appeared around 150, 160, and 177 amu/charge are noise.

Kinetic energy measurement of scattered ions. A kinetic energy distribution of scattered ions contains important information regarding the dynamics of RIS process. The energy distribution was measured by using an AEA together with a quadrupole mass filter, as described in Section (2.3). The energy distributions for scattered Cs^+ ions and CsH_2O^- cluster ions, the latter produced from an H_2O-covered surface, are presented in Figure 5. The energy was measured in energy increments of 0.2 eV, and the energy resolution of the analyzer was 1 eV in average over the examined range. Figure 5(a) shows the energy spectra of Cs^- ions scattered from a clean Pt(111) at incident energy of 30 eV. The incident and exit angles were both 70° to the normal of surface plane (specular scattering). The scattered Cs^- ions exhibit a rather sharp distribution with a prominent peak at 25 eV. The peak position indicates that the projectile ions transfer about 20% of initial energy to the surface in average. From the narrowness of the distribution we consider that the ions experience a relatively flat surface potential during the scattering, and that the effect of atomic corrugation on a Pt(111) surface is small.

Figure 5(b) corresponds to the case when Cs^+ scatters from an H_2O-covered Pt(111) surface. The surface was prepared by exposing 0.75 L of H_2O gas onto a sample maintained at temperature of 100 K. The H_2O exposure was done using a back-filling method to prepare a uniformly adsorbed layer.[25] The incident beam energy and the scattering angles were the same as in Figure 5(a). The energy spectra are shown for Cs^+ and CsH_2O^-. A change first noticed in the Cs^- energy spectrum obtained after H_2O adsorption is a decrease of scattered Cs^+ ion intensity by about 100 times compared with that on clean Pt(111) shown in Figure 5(a). The Cs^- intensity has now become comparable to the CsH_2O^+ intensity. Second, the energy distribution of Cs^- becomes very broad and has two maxima. The high energy maximum

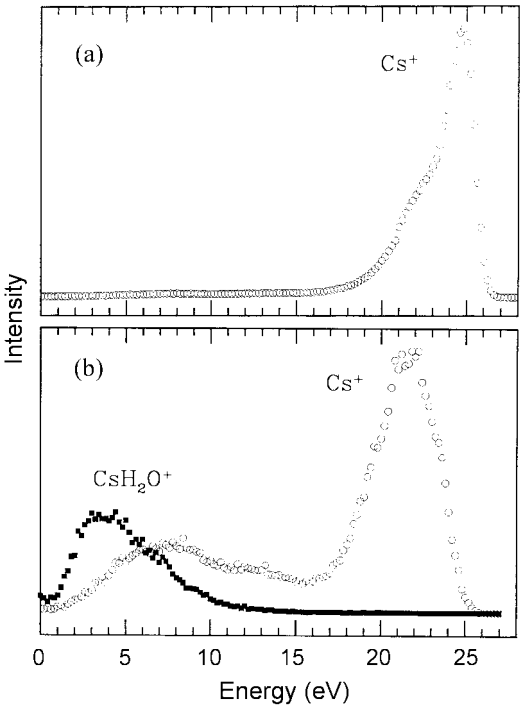

Figure 5. (a) Energy distribution of Cs^- ions scattered from a clean Pt(111) surface. (b) Energy distribution of Cs^- and CsH_2O^- scattered from a Pt(111) surface exposed to 0.75 L of H_2O at temperature of 100 K. The instrumental conditions were the same in (a) and (b): Cs^+ beam energy was 30 eV, incident and exit angles were both 70° with respect to the surface plane (specular geometry).

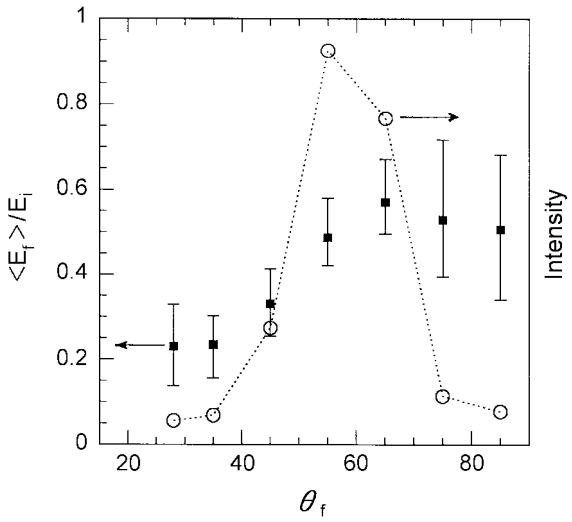

Figure 6. Angular distribution of the intensity (open circles) and the kinetic energy (solid squares) of scattered Cs^- ions. The energy is shown in a relative scale, *i.e.*, in the ratio of the final to incident energy (E_f/E_i). Cs^- beam was impinged to a clean Pt(111) surface with 30 eV at a fixed incident angle of 45°. The kinetic energy of scattered Cs^- ions was resolved by AEA. The amplitude of the error bars corresponds to the width of an energy distribution of scattered Cs^-.

appears at an energy near that of the elastically scattered Cs^+ in Figure 5(a). The maximum has shifted to a slightly lower energy after water adsorption, and the peak shape has also somewhat changed. Another maximum appears at a far lower energy (7-8 eV). These changes of the energy distribution must be due to H_2O adlayer on the surface. The energy distribution of CsH_2O^+ product peaks at 3-4 eV and tails to the high-energy side up to 10 eV. Apparently, the energy distribution of CsH_2O^+ overlaps largely with the low-energy component of Cs^-, suggesting that the two species may have a common origin. *i.e.*, CsH_2O^+ may be formed from low-energy Cs^-, and vice versa. On the other hand, Cs^+ ions under the high-energy envelope are not likely to combine with desorbed H_2O molecules because of large velocity mismatch between the two species.

Angular distribution of scattered ions. Angle-resolved measurements of Cs^- ions scattered from a clean Pt(111) surface are presented in Figure 6. The scattering conditions were Cs^+ beam energy of 30 eV and incident angle of 45°. We independently rotated a Cs^- gun and a sample around the z-axis as mentioned in Section (2.2), and detected Cs^- ions that were scattered into a QMS located on a plane of ion gun rotation. In other words, the experiment measured the angular distribution of the in-plane scattered Cs^- ions. The open circles in Figure 6 represent the angular dependency of scattered Cs^+ intensity. The Cs^- intensity was measured in two ways such that it is independent of scattered energy: (i) a total flux of scattered Cs^+ was measured with a QMS by detaching an AEA. (ii) An energy-distribution curve of Cs^- was measured in the presence of AEA, which was then energy-integrated to give a total flux. The both methods produced similar results for the angular distribution of Cs^-. The angular distribution peaks around 60° with respect to the surface normal. Since the beam incidence direction is 45°, the result indicates that Cs^+ tends to scatter toward a supraspecular direction.

The solid squares in Figure 6 are the average kinetic energies of Cs^- ions scattered to various angles, presented in the relative energy scale (E_f/E_i). The average energy was obtained from energy distribution curves (not shown), and the amplitude of the error bars corresponds to the width of the energy distribution. The data clearly show a trend of increasing energy as the ions exit toward a more glancing angle.

The preferential supraspecular scattering of Cs^- ions indicates that the surface potential that a projectile ion experiences during the collision is relatively flat. Due to a less corrugated surface potential, the ions do not efficiently lose energy in the surface-parallel direction and leave the surface with a momentum that is larger along this direction. This interpretation is also supported by the observation that ions indeed retain higher energy as they scatter in a more glancing angle. The features of Figure 6 have been successfully reproduced by a molecular dynamics (MD) classical trajectory calculation of Cs^- scattering on Pt(111).[26] The interpretation of the experimental data presented here is only preliminary. Yet, we would like to emphasize that the angular and energy distributions are the features most appropriate to and directly comparable with MD trajectory

simulation. Such experimental data, when aided by theoretical analysis, will be able to bring detailed understanding of the RIS process.

Acknowledgment. The work has been supported by the Creative Research Initiatives Project from MOST, Republic of Korea. The authors thank Professor J. A. Yarmoff (U. C. Riverside, USA) for useful discussions in the construction stage and the staffs of machine shop at Postech for technical assistance.

References

1. Kasi, S. R.; Kang, H.; Sass, C. S.; Rabalais, J. W. *Surface Sci. Rep.* **1989**, *10*, 1.
2. Cooks, R. G.; Ast, T.; Pradeep, T.; Wysocki, V. *Acc. Chem. Res.* **1994,** *27*, 316.
3. Wainhaus, S. B.; Gislason, E. A.; Hanley, L. *J. Am. Chem. Soc.* **1997**, *119*, 4001.
4. (a) Morris, Jr. M. R.; Riederer, D. E.; Winger, B. E.; Cooks, R. G.; Ast, T.; Chidsey, C. E. D. *Int. J. Mass Spectrom. Ion Processes* **1992**, *122*, 181. (b) Miller, S. A.; Luo, H.; Pachuta, S. J.; Cooks, R. G. *Science* **1997**, *275*, 1447.
5. Yang, M. C.; Lee, H. W.; Kang, H. *J. Chem. Phys.* **1995**, *103*, 5149.
6. (a) Yang, M. C.; Hwang, C. H.; Ku, J. K.; Kang, H. *Surface Sci.* **1996**, *366*, L719; (b) Yang, M. C.; Hwang, C. H.; Kang, H. *J. Chem. Phys.* **1997**, *107*, 2611.
7. (a) Kang, H.; Kim, K. D.; Kim, K. Y. *J. Am. Chem. Soc.* **1997**, *119*, 12002. (b) Kang, H.; Yang, M. C.; Kim, K. D.; Kim, K. Y. *Int. J. Mass Spectrom. Ion Processes* **1998**, *174*, 143.
8. Kim, K.-Y.; Shin, T.-H.; Han, S-J.; Kang, H. *Phys. Rev. Lett.* **1999**, *82*, 1329.
9. Han, S-J.; Park, S. C.; Lee, J.-G.; Kang, H. *J. Chem. Phys.* **2000**, *112*, 8660.
10. Park, S.-C.; Kang, H.; Lee, S. B. *Surface Sci.* **2000**, *450*, 117.
11. Hwang, C. H.; Lee, C. W.; Kang, H.; Kim, C. M. *Surface Sci.* in press.
12. Shin, T.-H.; Han, S.-J.; Kang, H. *Nucl. Instrum. Methods in Phys. Res. B* **1999**, *157*, 191.
13. (a) Kang, H.; Shin, T.-H.; Park, S.-C.; Kim, I. K.; Han, S-J. *J. Am. Chem. Soc.* **2000**, *122*, 9842. (b) Park, S.-C.; Meang, K.-W.; Pradeep, T.; Kang, H. *Angew. Chem. Int. Ed.* **2001**, *40*, 1497.
14. Choi, W. Y.; Kang, T. H.; Kang, H. *Bull. Korean Chem. Soc.* **1990**, *11*, 290.
15. MDC Vacuum Products (23842 Cabot Boulevard, Hayward, CA 94545-1651, U.S.A., webmaster@mdcvacuum.com).webmaster@mdcvacuum.com
16. Kimball Physics (311 Kimball Hill Road, Wilton, NH 03086-9742, U.S.A., info@kimphys.com).
17. ABB Extrel (575 Epsilon Drive, Pittsburgh, PA 15238, U.S.A., components@extrel.com).
18. Park, S.-C. *MSc. Thesis*: Pohang University of Science and Technology: 2000.
19. Kepco (131-38 Sanford Avenue, Flushing, NY 11352 U.S.A., hq@kepcopower.com).
20. Eurotherm (Unit 10, 40 Brookhollow Avenue, Baulkham Hills, NSW 2153, Austrailia, eurotherm@ eurotherm.com.au).
21. Keithley Intruments (28775 Aurora Road, Cleveland, OH 44139, U.S.A., info@keithley.com).
22. Weare, C. B.; Yarmoff, Y. A. *Surface Sci.* **1996**, *348*, 359.
23. Yarmoff, Y. A.; Weare, C. B. *Nucl. Instrum. and Methods in Phys. Res. B* **1997**, *25*, 262.
24. Thiel, P. A.; Madey, T. E. *Surface Sci. Rep.* **1987**, *7*, 211.
25. Brown, D. E.; George, S. M.; Huang, C.; Wong, E. K.; Rider, K. B.; Smith, R. S.; Kay, B. D. *J. Phys. Chem.* **1996**, *100*, 4988.
26. Lahaye, R. J. W. E.; Kang, H. *Surface Sci.* in press.